



Hydrodynamic Model-Based Evaluation of Sediment Transport Capacity for the Makhool-Samarra Reach of Tigris River

Ala H. Nama^{a,b*}, Ali S. Abbas^a, Jaafar S. Maatooq^a 

^a Civil Engineering Dept., University of Technology-Iraq, Alsina'a street, 10066 Baghdad, Iraq.

^b Department of Water Resources Engineering, University of Baghdad, Baghdad, Iraq.

*Corresponding author Email: bce.19.02@grad.uotechnology.edu.iq

HIGHLIGHTS

- Flow velocities within most of the Makhool-Samarra Reach of the Tigris River are considered high compared to the local and worldwide flow velocity ranges.
- Toffaleti sediment transport function with the Van Rijn fall velocity and the effective depth-to-width computation methods are the most compatible and suitable methods for computing the Sediment Transport Potential (STP) in the Makhool-Samarra Reach of the Tigris River.
- The computed STPs in the Makhool-Samarra Reach of the Tigris River are considered high on local and global scales, especially during high flow.
- Medium gravel is the larger grain gradation class that can be transported. However, the suspended sediment is the dominant part of the Sediment Transport Capacity (STC), with a great majority of clay and very fine silt.

ABSTRACT

This paper implemented an HEC-RAS-based steady two-dimensional hydrodynamic model to evaluate the hydraulic characteristics and Sediment Transport Capacity (STC) of the Makhool-Samarra Reach of the Tigris River, where this part is not already investigated. This model was prepared with the aid of topographical surveys, hydraulic measurements, and laboratory tests, as well as recorded data. The main findings show that the flow velocities within most of the studied reach are considered high compared to the local and worldwide flow velocity ranges in natural rivers. Also, the Toffaleti sediment transport function with the Van Rijn fall velocity and the effective depth-to-width computation methods are the most compatible and suitable methods for computing the Sediment Transport Potential (STP) in the studied reach. With the maximum flow, the computed STP was less than the average (5.7×10^6 tons/day) in 45% of the reach length, where the maximum STP is 8.7×10^6 tons/day. However, with the minimum flow, the STP intermittently fluctuates below the average (0.2×10^6 tons/day) in 48% of the reach length, where the minimum STP is 0.14×10^6 tons/day. Generally, these STPs are little more than the Tigris River in Mosul and much higher than that in Baghdad. Also, these STPs are considered high on a global scale, especially during high flow. Medium gravel is the larger grain gradation class that can be transported. It constitutes less than 0.00005 % of the STP. Furthermore, the STC computations clearly show that the suspended sediment is the dominant part of the STC and the bed material constitutes less than 0.002% of the STC of the total load. However, most of the STC concerns the clay and very fine silt.

ARTICLE INFO

Handling editor: Mahmoud S. Al-Khafaji

Keywords:

Hydrodynamic; Hydraulic aspects; Sediment transport Capacity; Tigris River; Makhool-Samarra

1. Introduction

Worldwide, water resource systems have experienced many inconsistencies due to climatic change and human interventions through the construction of hydraulic structures for different purposes. One of the most affected changes is the alteration of the morphology of natural rivers through erosion of river banks and floodplains or sediment deposition in the river. This may reduce the flood-carrying capacity, leading to floodwater damage to the surrounding area. Fluvial processes in natural rivers can be sufficiently predicted using basic sediment transport principles. The Sediment Transport Potential (STP), which is the transportable mass of particular grain classes in response to hydraulic parameters, and then the Sediment Transport Capacity (STC), which is the maximum sediment load, a particular discharge, can transport [12], are very important parameters of natural

river morphology. Many studies adopted the field and laboratory-based approach for investigating the STP and STC in natural rivers such as [3-10]. With the help of recent computer software, these parameters can be computed and evaluated using hydrodynamic-based sediment transport simulation models. The Hydraulic Engineering Center-River Analysis System (HEC-RAS) is one software that can help analyze the STC. In Iraq, [11-13] utilized the HEC-RAS software to investigate the effect of floating debris on local scour at bridge piers, evaluating the hydraulic performance indicators for Al- Ibrahim Irrigation Canal in the south of Iraq, and modeling micro-hydroelectric power plants utilizing artificial falls. Regarding the simulation and computation of STP and STC, [14] compared the measured and computed sediment concentrations. This comparison indicated that the commonly used Ackers and White, Engelund and Hansen, and Yang equations do not apply to large rivers. In contrast, Toffaleti's method reasonably estimates STC for large rivers. [15] implemented a one-dimensional hydraulic model to simulate the flow and compute the STC of the Tigris River in Mosul City. Whereas, in South Korea, [16] utilize the HEC-RAS to investigate the potential restoration of abandoned channels of the Mangyeong River. In addition, [17] compared the results of applying a quasi-unsteady HEC-RAS simulation model (QHRM) with that of a one-dimensional Finite Volume Method simulation model (FVMM) to predict the hydraulic and sediment transport parameters in the Pantano Wash River in Arizona, USA. The results indicated good agreement between the computed bed degradation and aggradation using the QHRM and FVMM. Also, for the QHRM, Yang's and Engelund-Hansen's equations gave the highest agreement between the measured and predicted values for this case study. [18] used an experimental flume data set to compute STC in HEC-RAS and to compare the computed and measured STC. The main finding showed that the Englund-Hansen and Ackers-White functions are applicable in the Soni River, Japan, and the computed sediment transport rates agree with the measured values. [19] implemented an HEC-RAS model, with the aid of a field topographical survey and ADCP field measurements, to determine the STC in a reach of the Euphrates River has a length of 6 km upstream of the Al-Shamia Barrage in the Al-Diwaniya City, Iraq. The main finding was that the England-Hansen formula was the best to predict the STC in the considered reach. [20] modeled the flow and computed the STC of the Tigris River in Baghdad, Iraq, using HEC-RAS. In this reach of the River, the Toffaleti sediment transport function was the most applicable. Through this computation, the location of low STC was specified. Also, [21] utilized the HEC-RAS software, using a set of field measurements, to estimate the flow characteristics and STC in Al-Abbasia Reach of the Euphrates River, Iraq. Locations of the low flow velocity and STC were specified. Furthermore, [22] used the HEC-RAS to study the same reach of the Tigris River in Baghdad that was investigated by [20], with the same geometric and flow data, to re-evaluate the STC of this reach and predict the changes in the river bed for the period 2012-2017. Moreover, [23] used an HEC-RAS model to simulate the flow and predict the STC upper reach of the Al-Gharraf River, which has a length of 58.2 km, in Kut, Iraq. Also, [24] used the HEC-RAS software to study the STC of Diyala River, Iraq.

The Makhool-Samarra Reach of the Tigris River in Salhaldien Governorate, Iraq, Figure 1, has a length of 130 km. It starts at the location of Makhool Dam, which is under construction, 30 km northwest of Baiji and about 15 km downstream from the confluence of the Lower Zab River with the Tigris River, and ends in Samarra Barrage [25]. This barrage plays the main role in diverting the excess water from the Tigris River to Tharthar Lake during the flood season [26]. The reach passes through many large cities and towns, such as Biji, Al-Alm, and Tikrit.

In the decades of the period 1931 to 1985, the flow in this reach was highly fluctuated [27]. However, a clear decrease in this fluctuation and flow amount occurred after the construction of the Mosul Dam upstream of the Makhool-Samraa Reach, as well as the decrease in inflow from upstream countries and the increase in water demand and losses due to population growth and climate change in Iraq.

The suspended and bed sediment load of Tigris River and its tributaries are trapped upstream of Mosul and Dokan Dams. The source of the sediment transported in the Makhool-Samraa Reach, in addition to the bed material of the river itself, is the catchment area of the river located between the Mosul and Makhool dams, the catchment area of uncontrolled Upper Zab River, and the catchment area of the Lower Zab River between Dokan Dam and the considered reach where the sediment load directly transports into Tigris River.

Although there are many studies concerning the investigation of the morphological and sediment transport aspects for various reaches of the Tigris and Euphrates Rivers in Iraq, these aspects in the Makhool-Samarra Reach of the Tigris River were still not investigated. However, specifying the hydraulic characteristics and the river's capacity to convey the flood wave safely is one of the most important characteristics of the river. Moreover, it plays a major role in the growth of islands and changing the morphological characteristics of this reach. Accordingly, it is a critical issue in flood risk management. Therefore, in this paper integration of field observations and a steady two-dimensional hydraulic model, utilizing the HEC-RAS software, Version 5.0.6 [28], were used to implement and run a simulation model to estimate the flow characteristics and the STC in the Makhool-Samarra Reach of Tigris River.

2. Material and Method

2.1 Field and Laboratory Work

The field works included surveying the geometry of study reach, Water Surface Elevation (WSE), flow velocity (V), and discharge (Q) measurement, as well as bed material, suspension, and bed load sediment sampling. In addition, cross-sectional survey work, WSE measurements, and visual-based identification of land cover for the river's main channel and floodplains at 20 Cross Sections (CSs) along the study reach as well as specifying the locations of bridges and other main features were conducted on Sept. 2021. In addition, cross-sectional survey data of previously surveyed 24 CSs by the Ministry of Water Resources, Iraq (MoWRI), in 2014 (MoWRI 2014, unpublished data) were officially requested and received to prepare a sufficient database for the river geometry, as shown in Figure 2.

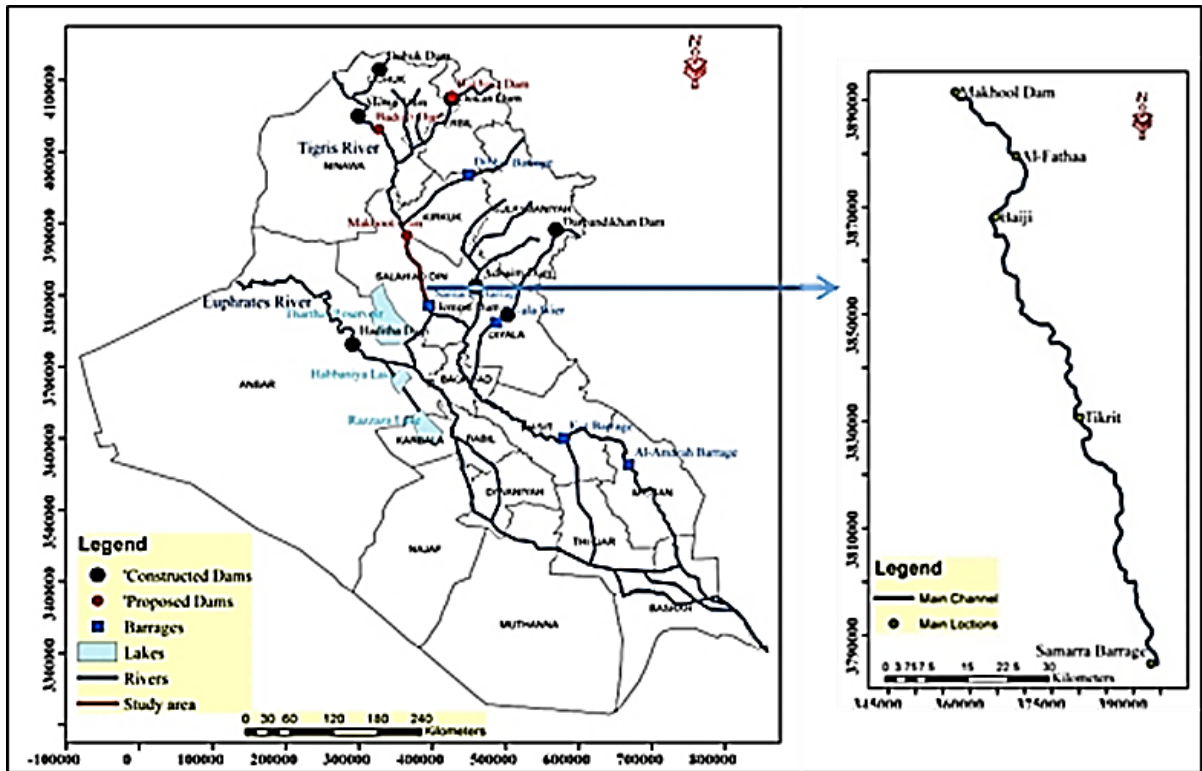


Figure 1: Makhool-Samarra Reach of Tigris River

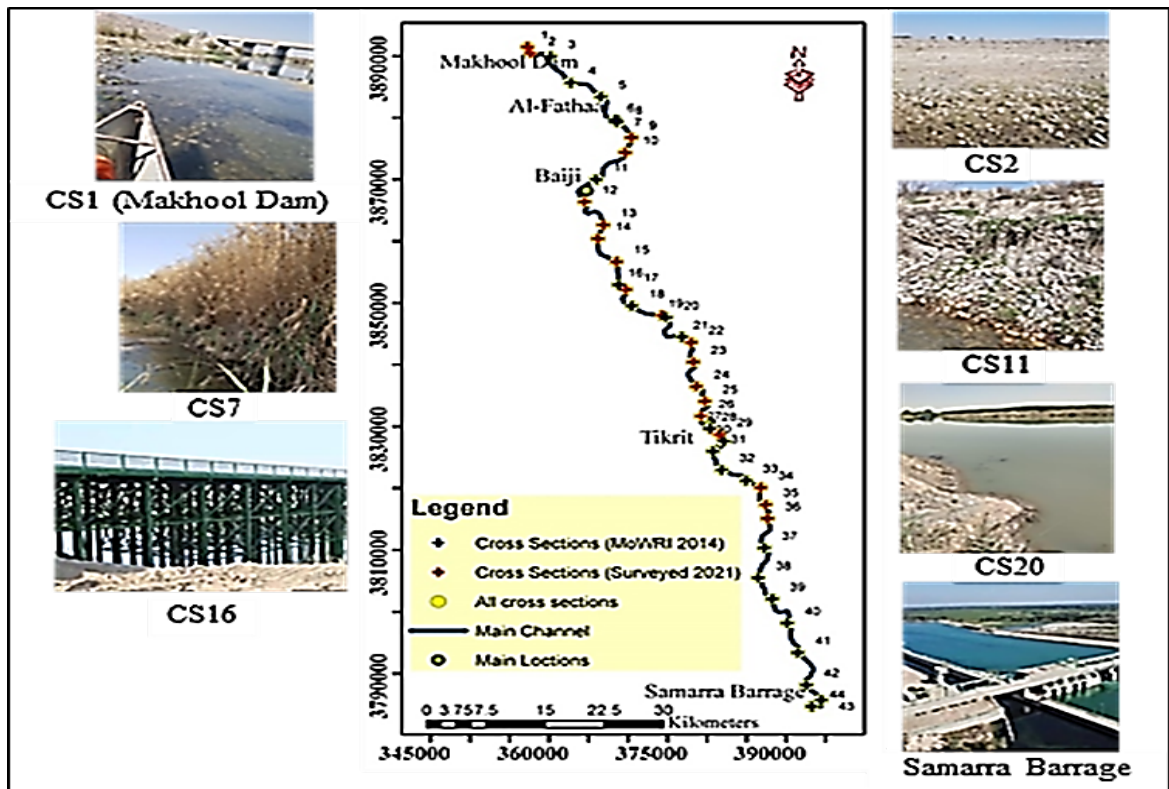


Figure 2: Location of field investigations

Furthermore, the recorded WSE at Samarra Barrage was also used. Moreover, two sets of V and Q were measured using the Acoustic Doppler Current Profiler (ADCP) M9 on 9 Sept. 2021 and 24 Feb. 2022. However, due to security conditions, these measurements were conducted only at 15 CSs from the surveyed 20 CSs.

In addition, monthly measurements for these flow parameters were conducted at the first cross-section (CS1), at the location of the proposed Makhool Dam, for the period 9 Sept. 2021 to 10 June 2022. It is worth mentioning that a high Q of $1197 \text{ m}^3/\text{s}$ was measured by MoWRI on 18 Dec. 2021.

To collect the bed material samples at the surveyed 20 CSs from 9 Sept. 2021 to 10 June 2022, a hand tool excavator and/or Van Veen Grab of 3.14 liters were used, according to the sampling position access conditions and particles sizes of the bed material. Sampling location, size, and method were specified according to the [29] guidelines. Thus, following the areal method for sampling, which gives grain size information from a small sampling area [30], three surface and sub-surface layer samples were collected at distances $1/4$, $1/2$, and $3/4$ of the average width for each cross-section. At the same distances, suspended and bed load samples were collected using a depth-integrating suspended sediment sampler and Helley-Smith bed load sampler, respectively. Two sets of these samples were collected on 9 Sept. 2021 and 24 Feb. 2022. Due to security conditions, these measurements were conducted only at 15 CSs from the surveyed 20 CSs. Furthermore, monthly sampling was conducted at CS1, at Makhool Dam, on 9 Sept. 2021, 21 Oct. 2021, 18 Nov. 2021, 29 Dec. 2021, 27 Jan. 2022, and 24 Feb. 2022, as well as 10 June 2022. In addition, a suspended load sample was taken concurrently with the measured high flow, $1197 \text{ m}^3/\text{s}$, at Baiji Station on 18 Dec. 2021. However, the flood conditions hindered the process of taking a bed load sample at that time.

2.2 Hydrodynamic Model

In the studied reach, with high, normal, and low flow conditions, there is no significant rapid change in inflow in terms of daily or even weekly inflow. Therefore, a steady two-dimensional flow hydraulic model can effectively simulate the flow in this reach to obtain the WSE, V , and sediment transport potential (STP) along the reach under steady flow conditions. To this end, the HEC-RAS software Version 5.0.6 was used. For the simulation of flow in rivers, the Navier-Stokes equations are utilized. These partial differential equations are numerically solved by combining the finite difference and finite volume numerical technique with a Newton's-like solution to compute the discrete solution for the hydraulic equations. However, this solution is based on the assumptions of incompressible shallow water flow, hydrostatic pressure, uniform density, and eddy viscosity used to approximate the turbulent motion for the assumed Reynolds averaged equations. Also, it is assumed that the horizontal length scales are much greater than the vertical scale [28].

The HEC-RAS model has four types of boundary conditions: known WSE, critical depth, normal depth, and rating curve. Specifying the suitable boundary conditions is based on the flow regime in the considered river. In HEC-RAS models, calibration involves calibrating the Manning's coefficient (n) values along the main channel and floodplains. This process can be performed by using initial values of n . These initial values are usually proposed following [31] and based on spatial information of land cover. A set of measured WSE and/or V is required to perform the calibration and validation process. However, some essential statistical indicators are used to evaluate the model performance. The coefficient of determination (R^2), Root Mean Square Error, Error-Observations Standard Deviation Ratio (RSR), and Nash-Sutcliffe coefficient (NS) are usually used as statistical indicators to evaluate the agreement between the computed and measured hydraulic parameters for the calibration and validation process. Generally, $R^2 > 0.6$, $RSR < 0.7$ and $NS > 0.5$ are satisfactory [32-36].

2.3 Computation of Sediment Transport Capacity (STC)

Computation of STP, which represents the transportable mass of particular grain classes in response to hydraulic parameters of the investigated channel, can be performed based on the results of the flow routing model. However, when using the HEC-RAS model for any cross-section, the STP can be computed using any of the following sediment transport equations; Meyer-Peter Müller, Yang, Wilcock, Ackers-White, Engelund-Hansen, Toffaletti or Laursen-Copeland. The selection of the appropriate equation depends on the conformity of the hydraulic and sediment properties of specified river sections with the criteria of this equation. For more details, see [28]. Once STP is computed, it should translate into the actual sediment gradation classes as a function of sediment composition. Subsequently, the Sediment Transport Capacity (STC), the maximum load of sediment that a given flow rate can carry, prorates the STP, reducing the transport of each grain class based on its prevalence in the sediment load [37, 38]. To investigate the entire range of the expected flow in the river reach, the results of hydraulic simulation for the case of maximum, average, and minimum flow were considered in STP computations. Based on the results of STP, sediment discharge rating curves can be developed for each cross-section. These curves help to understand the fluvial process in the considered river reach and identify the location of the critical part in terms of STP. Thus, the necessary remediation can be recommended.

3. Results and Discussion

3.1 Results of Field and Laboratory Work

The measured WSE, V , Q , and visual-based identification of n for the river's main channel and floodplains at the 15 CSs along the study reach on 9 Sept. 2021 and 24 Feb. 2022 are listed in Table 1. In addition, the monthly measurements for these flow parameters at the CS1, at the location of the proposed Makhool Dam, for the period 9 Sept. 2021 to 10 June 2022, are listed in Table 2. Finally, it is worth mentioning that a high Q of $1197 \text{ m}^3/\text{s}$ was measured by MoWRI on 18 Dec. 2021.

These measurements show that the water surface's slope ranges between 0.0001 and 0.0019, starting with a low slope from the beginning of the reach at the location of Makhool Dam to the location of Al-Fathaa at station 18.9 km. The proposed initial values of n were 0.035-0.029, where the left and right banks have high values. However, the measured flow velocities ranged between 1.9 and 0.4 m/s, where the highest velocity was measured at station 36.4 km downstream of the Baiji station by 2.5 km.

The measured discharges at the dam site were 425 and 475 m³/s. These discharges decrease along the river reach due to water consumption for various purposes by about 0.16 to 0.14, respectively.

The collected samples of bed material, suspended, and bed load were tested in the soil physics laboratory at the University of Baghdad, Iraq. The particle size distributions of the bed material for the surface layer samples were analyzed using sieving only without a hydrometer because the percentage of fine materials that pass the sieve 0.025 mm diameter is less than 10% for all tested samples, as shown in Figure 3a-i. However, the particle size distributions of the suspended and bed load are shown in Figure 4a,b.

Table 1: Hydraulic measurements along the river reach

CS	Distance (km)	WSE (m.a.s.l.)	Date						
			9 Sept. 2021			24 Feb. 2022			
			Manning's coefficient (n), based on visual identification of land cover shown in Figure 2.			V (m/s)	Q (m ³ /s)	V (m/s)	Q (m ³ /s)
			Right bank	Main Channel	Lift bank				
1	0.0	109.3	0.030	0.030	0.030	0.4	425.0	0.6	475.0
2	2.0	108.8	0.035	0.030	0.035	0.7	423.5	0.7	473.5
3	23.4	107.3	0.035	0.030	0.035	1.0	422.0	0.5	472.0
4	28.2	104.9	0.030	0.030	0.032	1.0	420.5	1.0	470.5
5	33.9	102.6	0.035	0.030	0.032	1.4	419.0	1.9	469.0
6	36.4	100.2	0.040	0.030	0.032	1.7	412.9	1.7	462.9
7	37.1	98.9	0.040	0.030	0.034	1.2	406.9	1.0	456.9
8	38.7	97.1	0.040	0.030	0.034	1.0	400.8	1.0	450.8
9	46.5	94.4	0.035	0.030	0.034	0.5	394.8	0.7	444.8
10	56.2	89.3	0.030	0.030	0.032	0.9	388.7	0.6	438.7
11	63.8	86.3	0.030	0.030	0.030	0.9	382.6	1.0	432.6
12	67.1	84.4	0.030	0.030	0.030	1.1	376.6	1.2	426.6
13	71.7	82.1	0.030	0.030	0.030	0.5	370.5	0.9	420.5
14	74.5	80.7	0.030	0.030	0.030	0.6	364.4	0.6	414.4
15	77.1	79.2	0.030	0.030	0.030	0.7	358.4	0.7	408.4
16	78.6	78.8	0.030	0.029	0.030				
17	80.5	78.0	0.030	0.029	0.030				
18	91.9	76.0	0.030	0.029	0.030				
19	95.9	75.0	0.030	0.028	0.030			Not measured	
20	100.7	72.0	0.030	0.028	0.030				
21	129.1	68.0	Samarra Barrage						

Table 2: Measured flow velocity and discharge at CS1

Date	V (m/s)	Q (m ³ /s)	Water surface elevation at Samarra Barrage (m.a.s.l.)
9 Sept. 2021	0.4	425	68.28
21 Oct. 2021	0.5	429	68.40
18 Nov. 2021	0.7	469	68.14
29 Dec. 2021	0.5	425	68.06
27 Jan. 2022	0.6	462	68.30
24 Feb. 2022	1.2	475	68.10
10 Jun. 2022	0.4	588	68.18
Average		468	68.20

3.2 Implementation of The Hydrodynamic Model

The essential step in preparing the hydraulic model is to input the geometrical data. They surveyed 20 CSs on Sept 2021 and received data from 24 CSs from MoWRI (2014). Visual-based identification of land cover on Sept 2021, as well as locations of bridges and other main features of the considered reach, were used to represent the river geometry. The visual-based identification of land cover, as shown in Figure 2 and Table 1, was adopted to propose the initial values of Manning's coefficient (n) for the main channel and floodplains following the classification proposed by [31]. Thence, these values are modified during the model calibration stage. The geometric data of all bridges on the river were involved in the model. As the flow regime in the considered reach is always subcritical, the boundary conditions were represented by the flow at the upstream and the known WSE at the downstream end. The recorded maximum and minimum Q, measured high Q, and the other four cases of the measured Q during the study period with corresponding WSE at Samarra Barrage were used to investigate the flow aspects along the river reach. These cases are listed in Table 3.

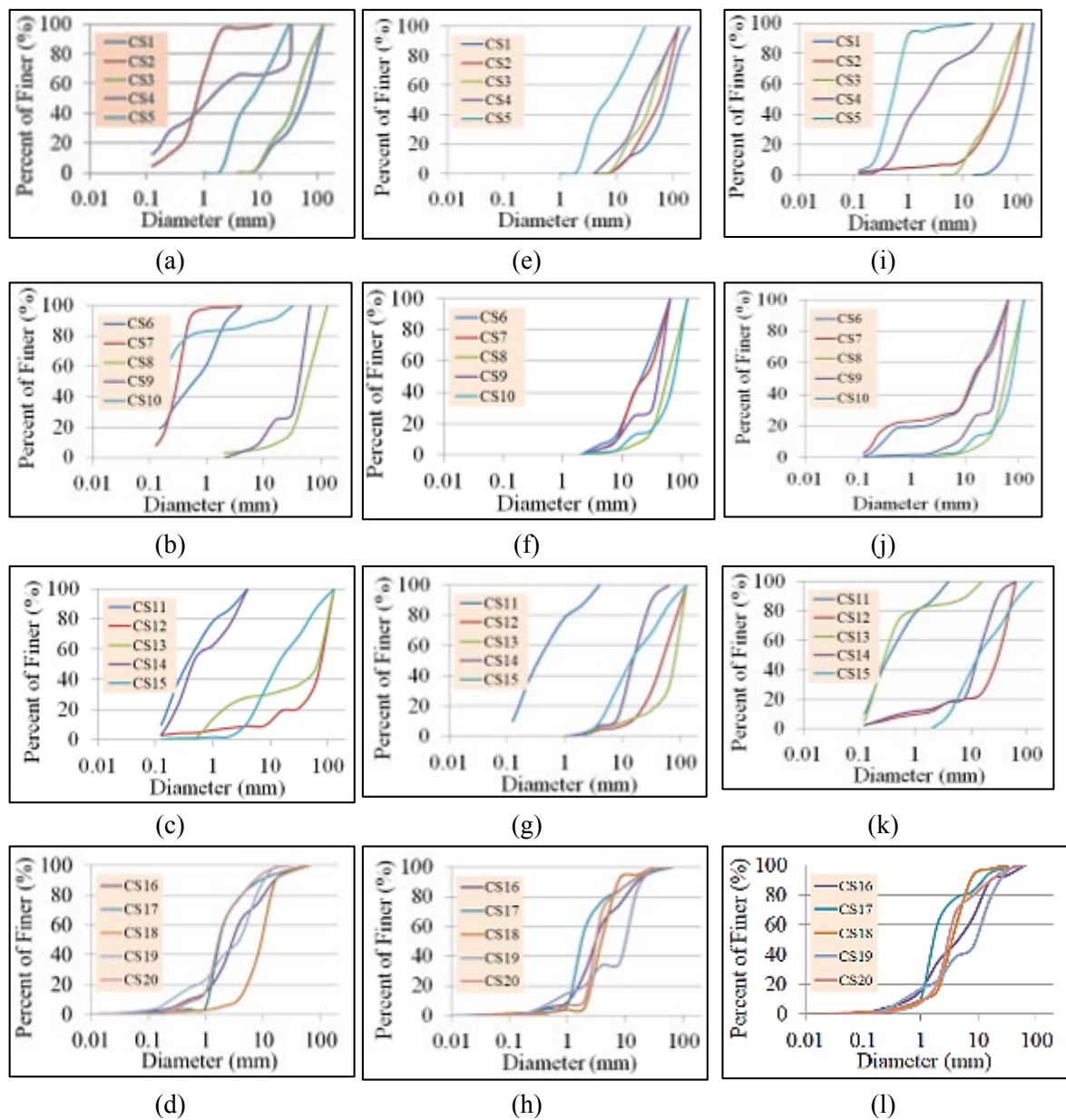


Figure 3: Grain size distribution of bed material: (a-d) for left bank; (e-h) for main channel; (i-l) for right bank

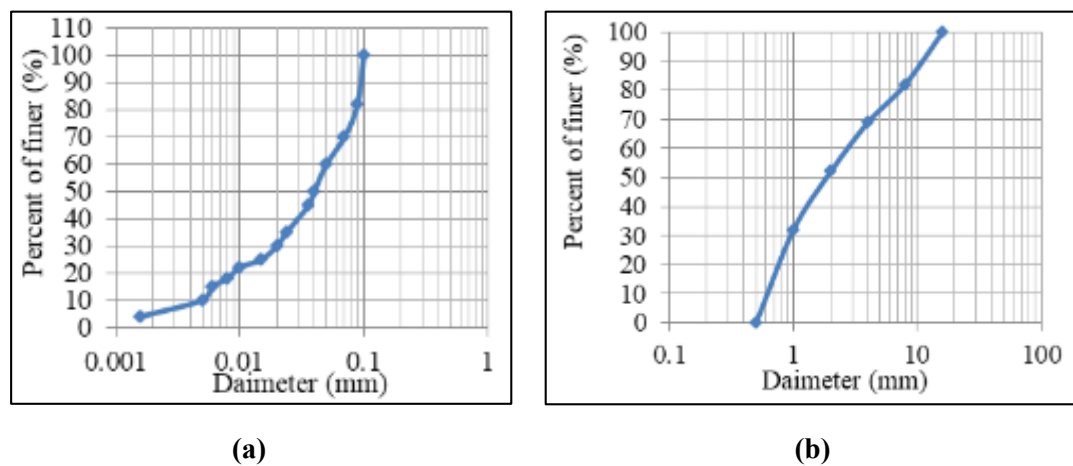


Figure 4: Grain size distribution of suspended and bed load: (a) suspended load, (b) bedload

3.3 Model Calibration and Validation

The model calibration and validation process were performed based on the observation during the normal flow conditions. This is because it is very difficult to perform hydraulic measurements along the studied river reach with the propagations of flood waves. Therefore, the R^2 , RSR, and NS were used to determine the hydraulic parameters in the calibration process and evaluate the model validation. The calibration process involved calibrating Manning's n values along the main channel and floodplains. As mentioned previously, this process was performed by using the initial values of n , proposed following [31], and based on the visual-based identification of land cover during the field survey works, as shown in Figure 5. To this end, the measured Q and the corresponding WSE at Samarra Barrage of Case 2, as listed in Table 3, were used as upstream and downstream boundary conditions. In addition, the measured WSE at the surveyed 20 CSs along the river reaches on the same date, as listed in Table 1, was used to determine the difference between the measured and computed WSE for evaluating the model performance. After many trials, the calibration process results show that when n values were, as shown in Figure 5, a high agreement between the measured and computed WSE, as shown in Figure 6, is obtained with R^2 , RSR, and NS of 0.87, 0.004 and 0.72 respectively.

Table 3: Adopted flow cases

Case No.	Description	Q (m ³ /s) At Makhool Dam	At Baiji Station		WSE (m.a.s.l.) at Samarra Barrage	Date
			Q (m ³ /s)	WSE (m.a.s.l.)		
Case 1	Minimum (MoWR 2021)	292	286	101.90	67.00	8 July 2021
Case 2	Normal Flow (for Model Calibration)	425	419	102.60	68.28	9 Sept 2021
Case 3	Normal flow (for Model Validation)	475	496	102.66	68.10	24 Feb 2022
Case 4	Average flow	469	463	102.62	68.14	18 Nov 2021
Case 5	Normal flow	588	582	102.9	68.18	10 June 2022
Case 6	High flow during the study period	1203	1197	103.8	68.10	18 Dec 2021
Case 7	Maximum (MoWR 2021)	11577	11571	107.6	69.0	12 Apr 2019

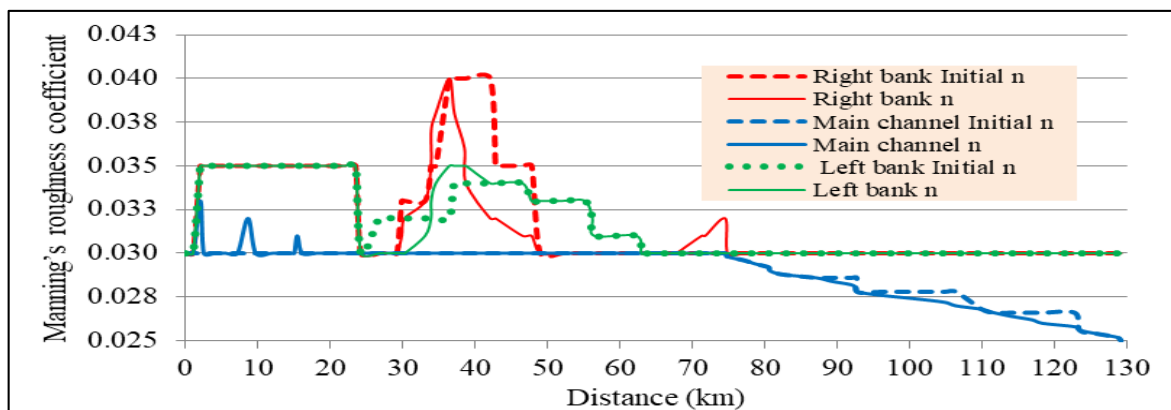


Figure 5: Initial and calibrated values of Manning's roughness coefficient (n) for the main channel and floodplains

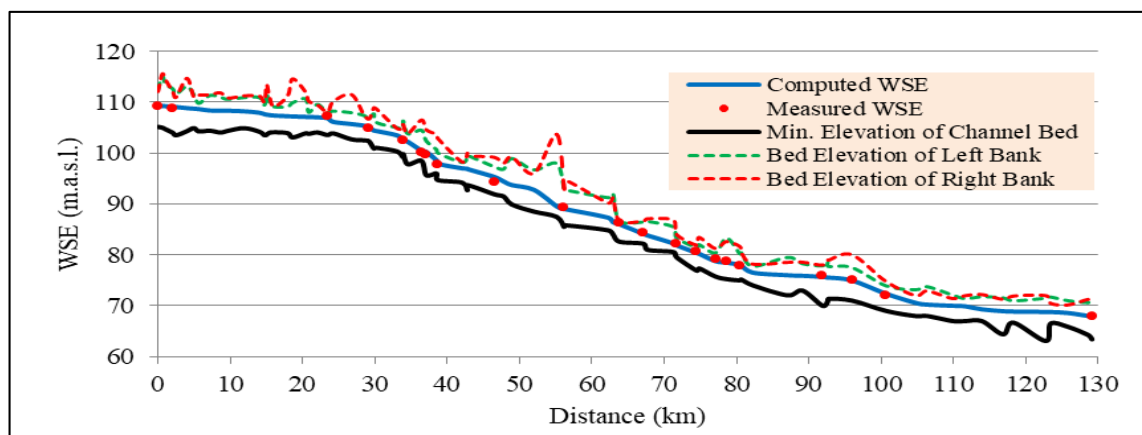


Figure 6: Computed and measured WSE along the river reach for Case 1

On the other hand, the measurement and computation-based rating curve at Baiji Station for Cases 1 to 7, which is listed in Table 3, and the measured V on 24 Feb 2022 at 15 CSs, which is listed in Table 1 with those computed for Case 3 which listed

in Table 3 were used to perform the validation process. The rating curve-based validity evaluation indicated an acceptable validity level with R^2 , RSR, and NS of 0.91, 0.17, and 0.90, respectively, as shown in Figure 7. As illustrated in Figure 8, the V-based validity evaluation shows an acceptable agreement between the measured and computed velocity with R^2 , RSR, and NS of 0.80, 0.54, and 0.71, respectively.

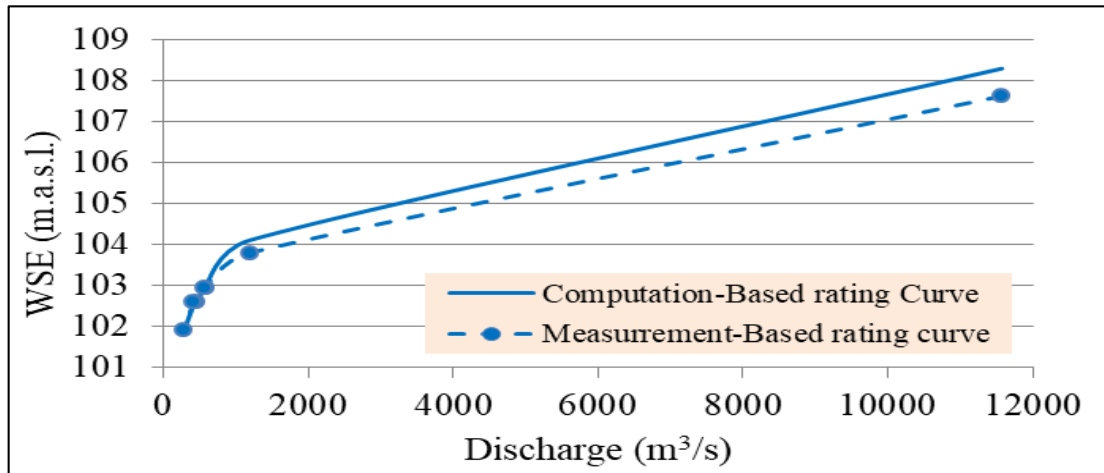


Figure 7: Measurement and computation-based rating curve at Baiji Station

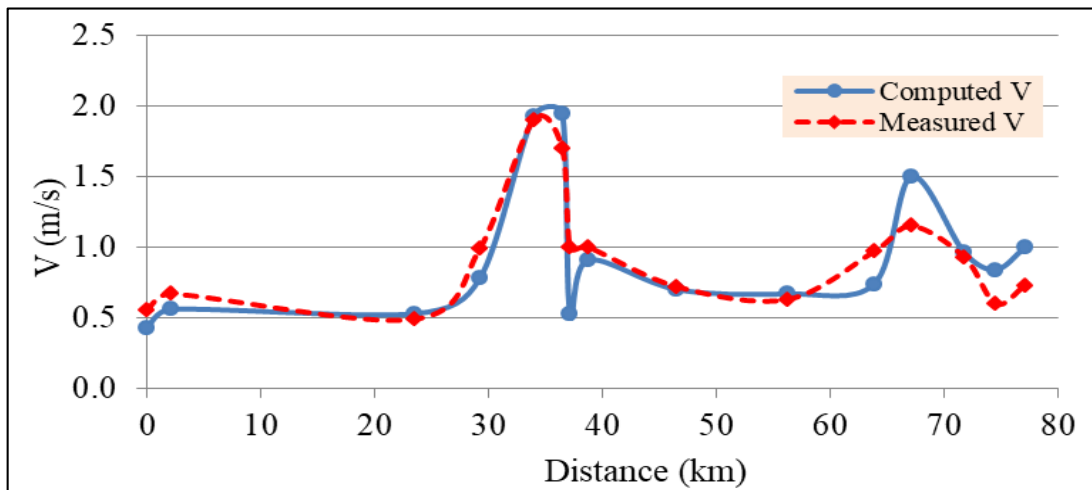


Figure 8: Measured vs. computed V on 24 Feb 2022 at 15 CSs

3.4 Hydraulic aspects

Application of the hydrodynamic model for cases 1 to 7 shows that the WSE along the considered reach was as illustrated in Figure 9. The maximum (minimum) WSEs at the Makhool Dam, Tikrit Bridge, and Samarra Barrage are 117.4 (108.6) and 84.1 (78.1), and 71 m.a.s.l. (67 m.a.s.l.), respectively. For the case of minimum flow ($292 \text{ m}^3/\text{s}$), the top width of the river in most of the reach before the station 113.9 km (located near the intake of Tigris Irrigation Project) fluctuated between 83.5 m at station 38.5 km (at the Al-Hajjaj district), and 847.4 m at station 55.1 km (At the pumping station of Al-kuzamiha irrigation project), while this width increases after the station 113.9 to be 2661 m near Samarra Barrage, Figure 10a-c.

In the case of maximum flow ($11577 \text{ m}^3/\text{s}$), this width distinctly increases to fluctuate between 521.9 m at station 18.6 km (at the Al-Fathaa), 5012.6 m at station 42.0 km (at Tal Sibab Village) and 1128.5 at station 104.7 (at the intake of Al-Dour Irrigation Project) and then it increases more to be 5260.3 m near the Samarra Barrage. According to the topographical and geological state of the reach basin, most of the large increase in top width is concentrated in the parts 28.5 to 50.0 km and 72 to 114 km of the reach. However, the maximum, average, and minimum flow velocities in the case of the maximum (minimum) discharge were 4.17 (3.2), 1.76 (0.76), and 0.6 m/s (0.09 m/s), respectively, Figure 11.

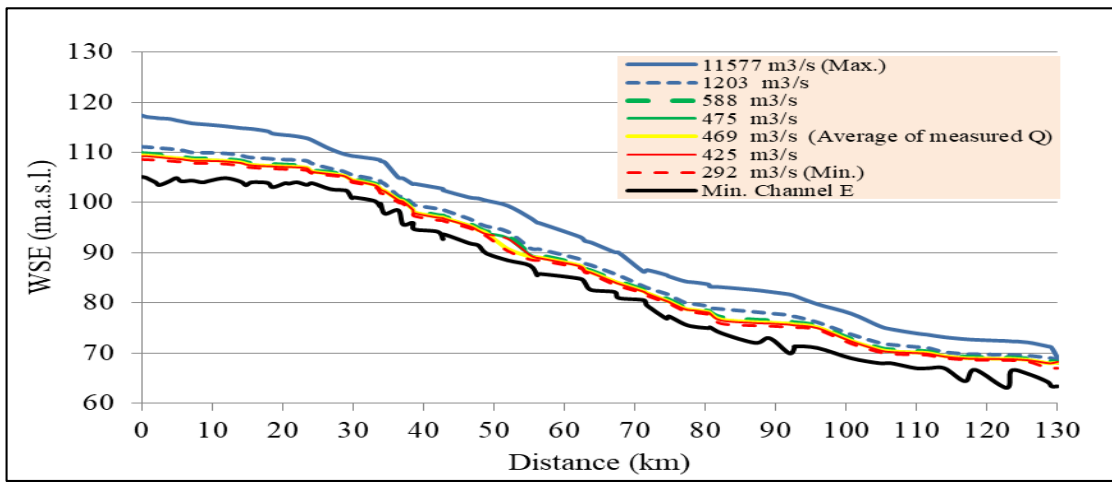


Figure 9: Computed WSE along the river reach

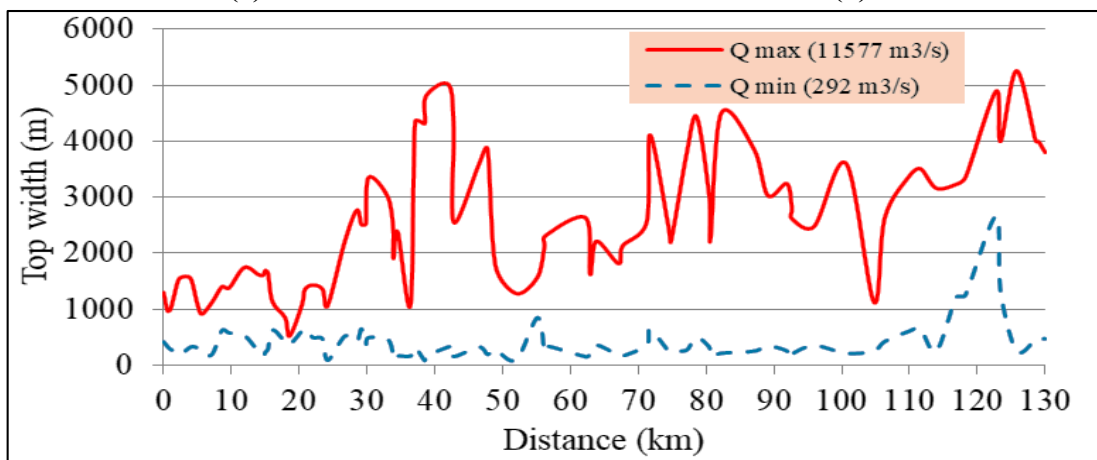
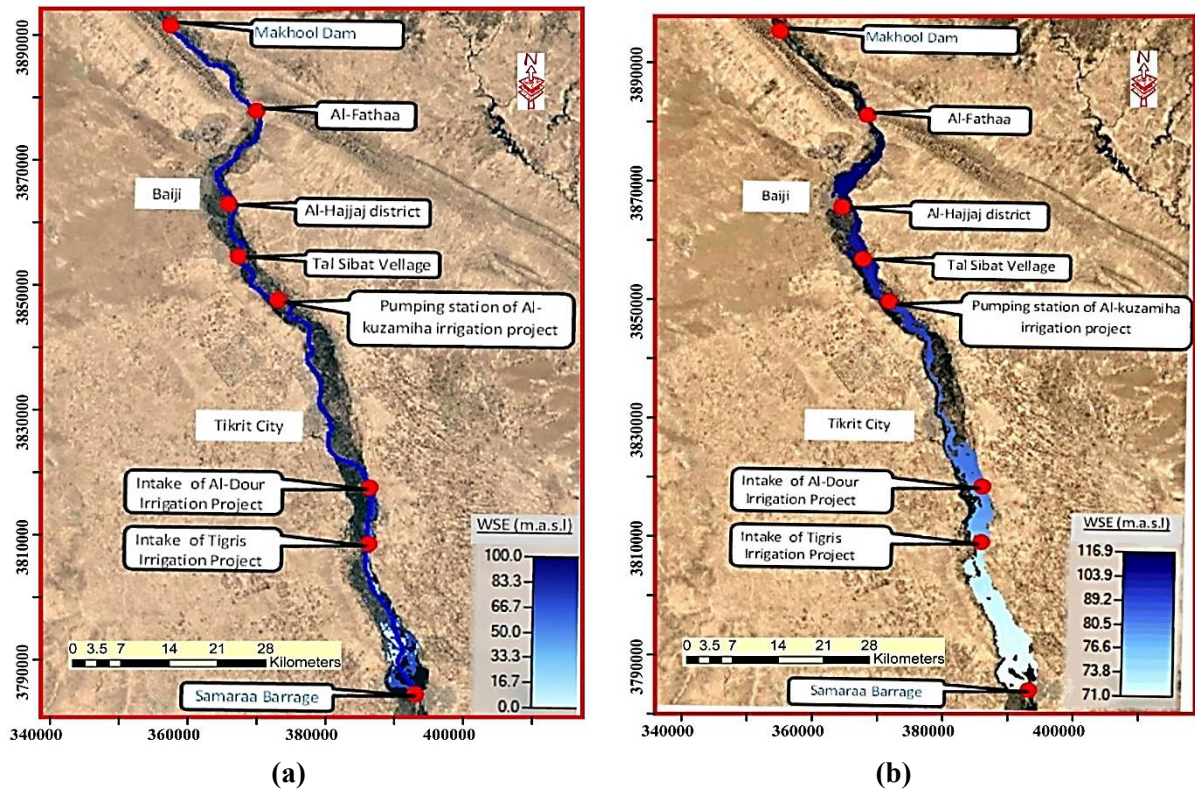


Figure 10: Computed top width along the river reach: (a) distribution of top width for the case of minimum flow, (b) distribution of top width for the case of maximum flow, (c) top width along the river reach

In general, these velocities are pretty much equal to that computed in the Tigris River within Mosul City [15]. However, they are much higher than that computed in the Tigris River reaches from Samarra to Baghdad and within Baghdad City by [20, 22, 39].

[40, 41] showed that in natural rivers, flow velocity greater than 2-3 m/s rarely occurs in nature. Hence, the measured and computed flow velocity in most of the Makhool- Samarra Reach are considered high compared to the worldwide and local range of river flow velocity such as that obtained by [15, 20- 22, 24].

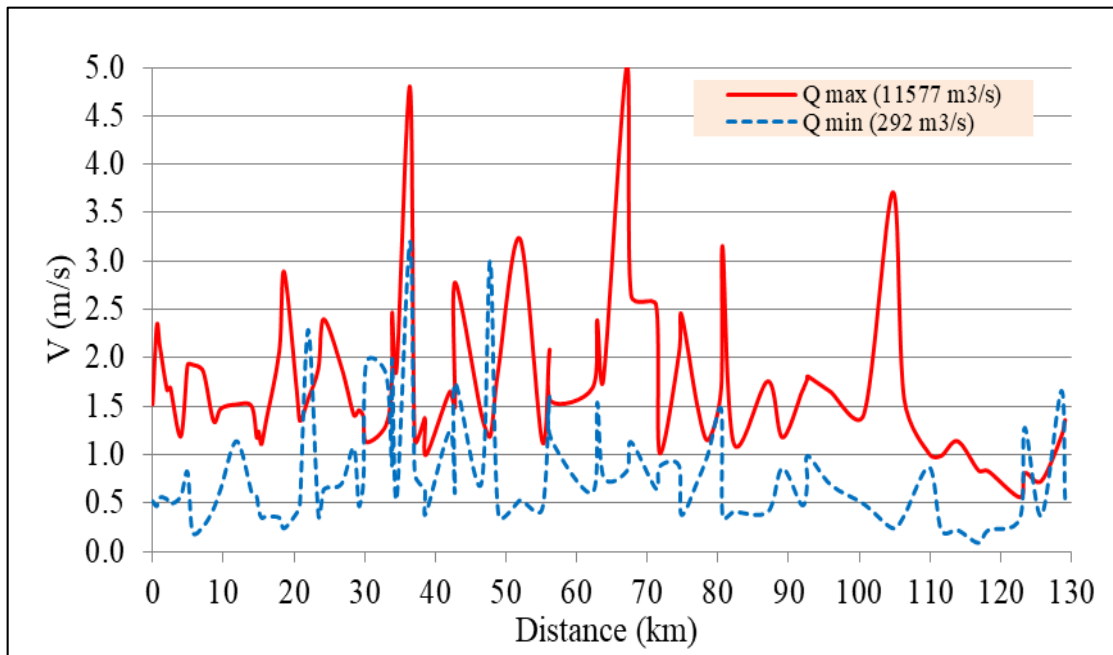


Figure 11: Computed maximum and minimum V along the river reach

3.5 Sediment Transport Potential (STP)

Comparing the results of the hydrodynamic model and the gradation of bed material, bed load, and suspended load with the criteria of the sediment transport functions indicated that only the Toffaleti sediment transport function, presented in [42], is compatible with the measures of the studied reach. This agreed with the recommendation of [11] for large rivers. Also, the Van Rijn fall velocity computation method [43] and effective depth-to-width hydraulic parameters computation method are the most suitable methods for computing the STP in the considered reach. Thus, the computed STP for the cases of maximum (11577 m³/s), average (469 m³/s), and minimum (292 m³/s) flow is shown in Figure 12.

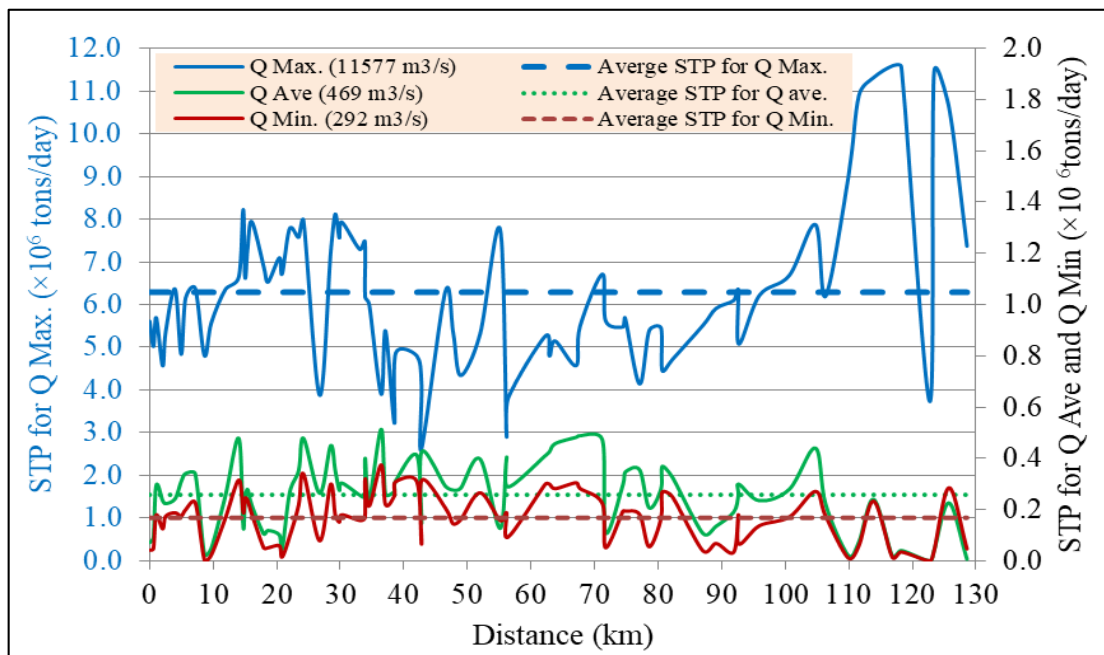


Figure 12: Computed STP for the maximum average and minimum flow

For the maximum discharge during the flood event, the maximum, average, and minimum STP are 11.6×10^6 , 6.3×10^6 , and 2.6×10^6 tons/day, respectively. The maximum STP occurs partly from station 116.8 km to station 118.3 km, approximately 11 km before the Samarra Barrage. In contrast, the minimum occurs between stations 42.8 and 46.5 km near the Al-Hajjaj District. For this discharge case, the computed STP was less than the average in 62% of the reach length. The low STP mainly extends along to parts of the reach. The first has a length of 11.9 km, starting at the Makhool Dam and ending at 10 km before the Al-Fathaa Bridge. In contrast, the second has a length of 62 km, starting at the Baiji Hydrological Station and ending at the inlet of the Tigris Irrigation Project.

For the measured average discharge during the study period (469 m³/s), the maximum, average, and minimum STP were 0.5×10^6 , 2.5×10^6 , and 1.3×10^3 tons/day, respectively. The maximum STP occurs at station 36.6 km near Baiji Hydrological Station. In contrast, the minimum occurs at station 122.7 km, about 7 km before the Samarra Barrage. The computed STP intermittently fluctuated below the average in 41% of the reach length. However, for the minimum flow (292 m³/s), the maximum, average, and minimum STP were 0.4×10^6 , 0.2×10^6 , and 0.14×10^3 tons/day, respectively. Similar to the measured average discharge, the STP intermittently fluctuated below the average but in 48% of the reach length, and the minimum occurs in the same part of the reach. The maximum STP occurs at Station 36.4, about 0.7 km after the Al-Baiji Village.

The STP rating curves of the aforementioned critical locations are shown in Figure 13. For the normal flow conditions, from the minimum (292 m³/s) to the highest measured discharge during the study period (1203 m³/s), station 36.4 km has the highest STP, and station 122.7 km has the lowest STP. However, although the STP of all stations sharply increased during the flood, the STP of station 14.7 km increased more sharply to be higher than that of station 36.4 km.

Generally, the STP of the considered reach for the cases of maximum, average, and minimum flow is little more than that of the Tigris River in Mosul, which was computed by [15], and a lot higher than that of the Tigris River in Baghdad, which computed by [20, 22] and. In terms of worldwide rivers and based on [3, 7, 17], the Makhool-Samarra Reach has a high sediment transport potential, especially during the high flow.

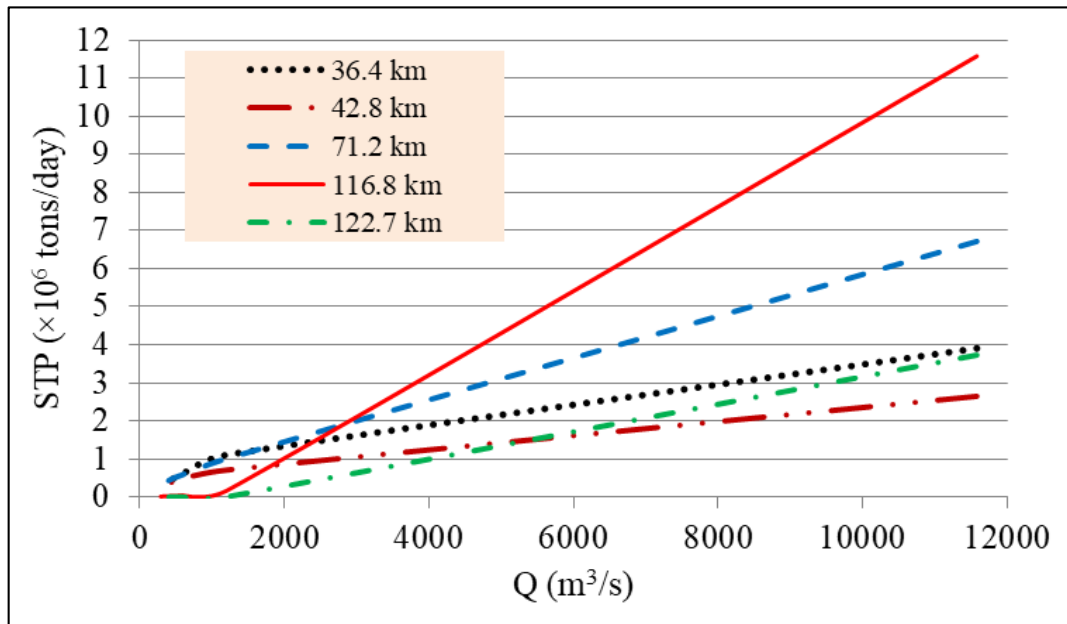


Figure 13: STP rating curves of the critical locations

3.6 Sediment Transport Capacity (STC)

Using the implemented HEC-RAS model, the larger grain gradation class that can be transported in the river reach with the minimum and maximum flow was investigated, as well as determining the reach STC of the clay class, which is the smallest gradation class. Figures 14 and 15 of this investigation show that the larger grain gradation class that can be transported is the Medium Gravel (MG). The STC of this class represents less than 0.00005 and 0.00004% of the STC of the clay class for the minimum and maximum flow cases. However, through adopting the gradation of the suspended and bed load, Figure 4, the computed STC of the suspended and bed load for the cases of minimum and maximum flow was shown in Figures 16 and 17.

These figures clearly show that the suspended sediment is the dominant part of the STC and the bed load constitutes less than 0.002% of the STC of the total load. However, the percentages of STC for the Clay, Very Fine Silt (VFM), Fine Silt (FM), Medium Silt (MM), Coarse Silt (CM), Very Fine Sand (FVS), Coarse Sand (CS), Very Coarse Sand (VCS), Very Fine Gravel (VFG), Fine Gravel (FG) and Medium Gravel (MG) classes of the sediment gradation for the cases of minimum and maximum flow were as shown in Figures 18 and 19. These percentages indicated that a large percentage, approximately 90%, of the STC concerns the Clay and VFM.

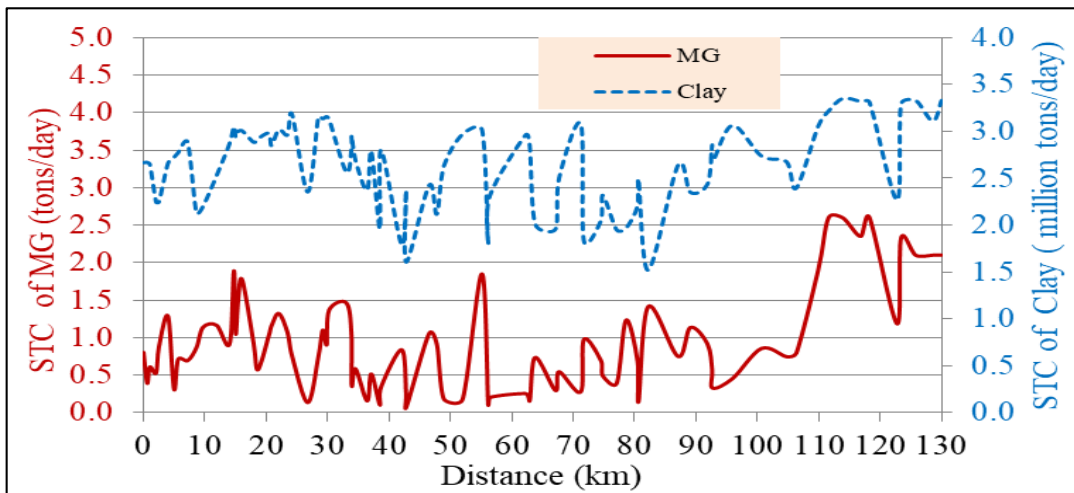


Figure 14: STC of the Clay and MG classes for the case of maximum flow (11577 m³/s)

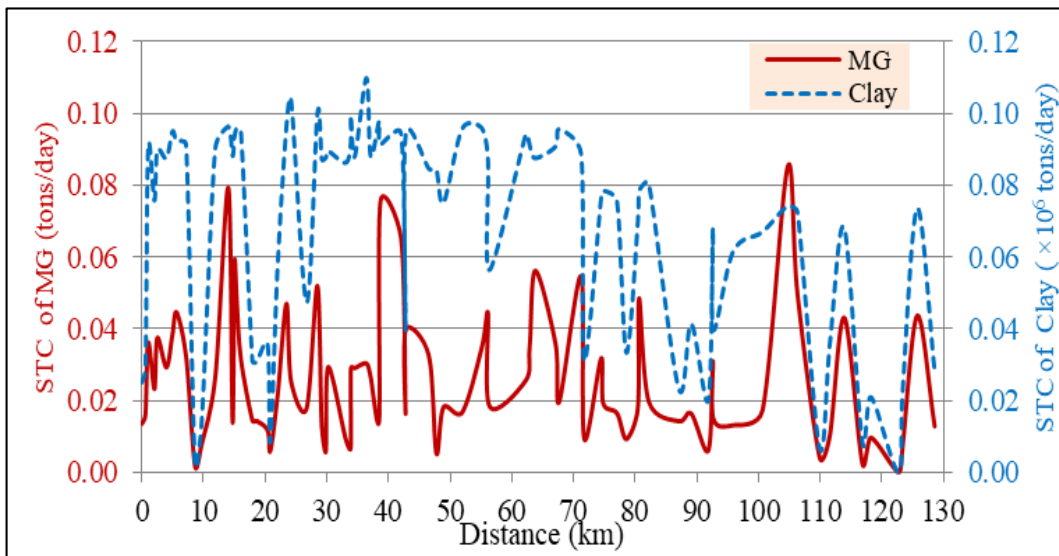


Figure 15: STC of the Clay and MG classes for the case of minimum flow (292 m³/s)

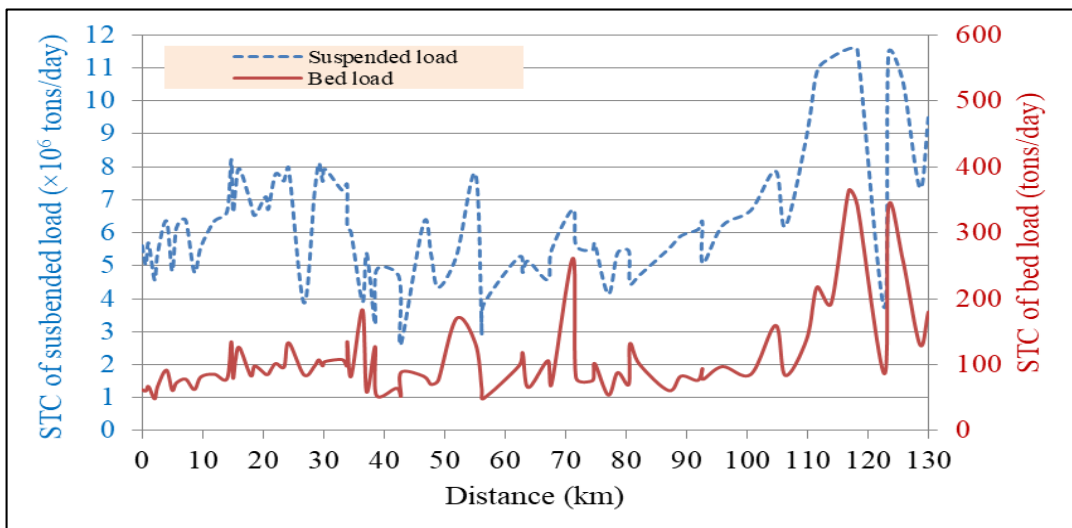


Figure 16: STC of the suspended and bed load for the case of maximum flow (11577 m³/s)

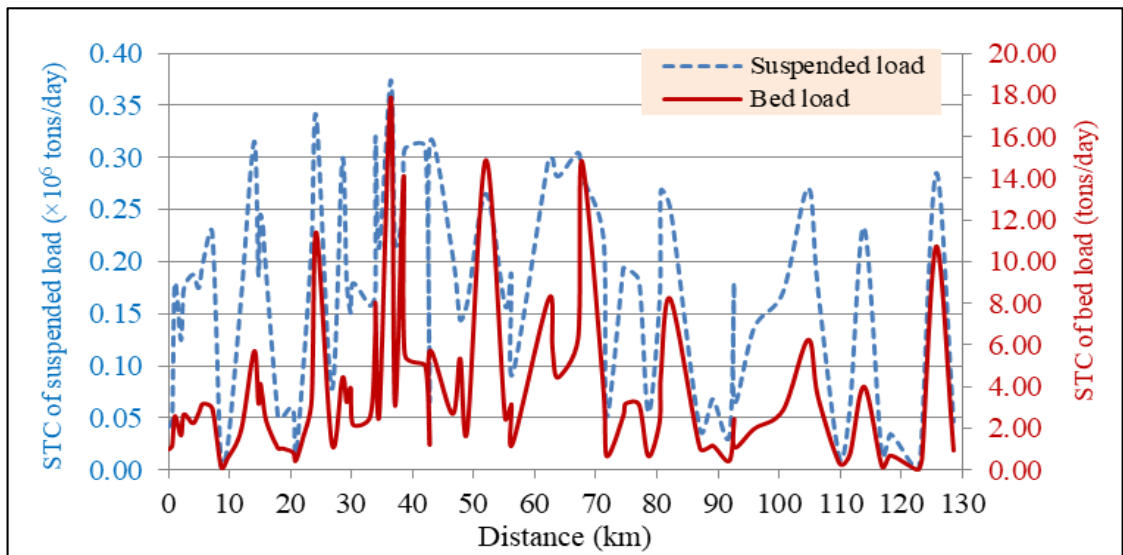


Figure 17: STC of the suspended and bed load for the case of minimum flow (292 m³/s)

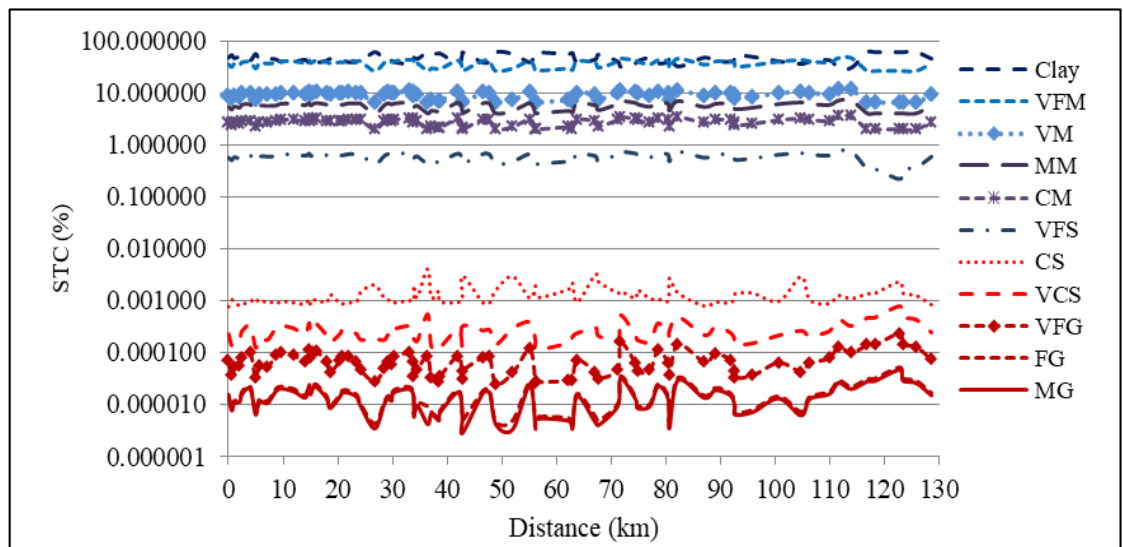


Figure 18: STC of the sediment gradation classes for the case of maximum flow (11577 m³/s)

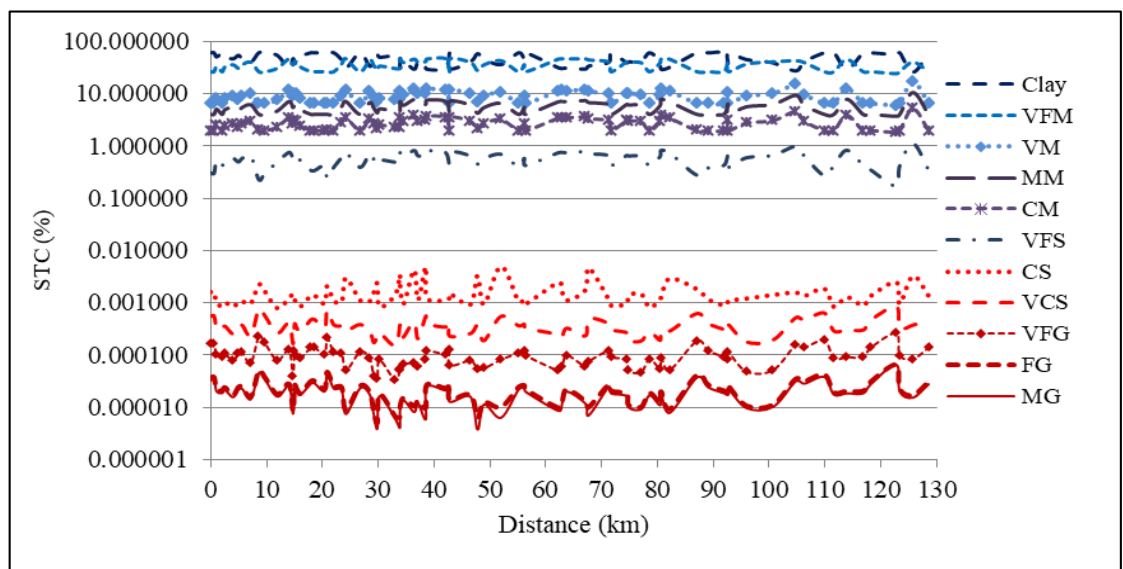


Figure 19: STC of the sediment gradation classes for the case of minimum flow (292 m³/s)

4. Conclusions

The Sediment Transport Capacity (STC) is one of the natural rivers' most important morphological aspects. It has a major role in increasing or decreasing the area of the river course and thus in changing the river's ability to pass flood waves. This paper evaluated the hydraulic characteristics and the STC of Makhool-Samarra Reach of the Tigris River, where this part is not already investigated. This evaluation was based on preparing and implementing a steady two-dimensional hydrodynamic model using the HEC-RAS software. The data required for this model was prepared by conducting topographical field surveys, hydraulic measurements, and laboratory tests, in addition to the data recorded by the competent directorates in the MoWRI. The main findings show that the flow velocities within the considered reach are generally equal to that in the Tigris River within Mosul and much higher than that in the reaches from Samarra to Baghdad and Baghdad. Moreover, in most of the reach parts, these velocities are considered high compared to the local and worldwide flow velocity ranges in natural rivers.

Concerning the STC, Toffaleti sediment transport function is the most compatible function with the measures of the studied reach. Also, the Van Rijn fall velocity computation method and the effective depth-to-width hydraulic parameters computation method are the most suitable methods for computing the Sediment Transport Potential (STP). The maximum STP, with the maximum discharge during the flood event (11577 m³/s), was less than its average in 62% of the reach length, and it is 11.5×10^6 tons/day, which occurs at 11 km before the Samarra Barrage. However, the minimum STP, with the minimum flow (292 m³/s), intermittently fluctuated below its average in 52% of the reach length and is 0.3×10^3 tons/day. This minimum STP occurs between stations 42.8 and 46.5 km near the Al-Hajjaj District. Generally, the STP of the considered reach for the cases of maximum and minimum flow is slightly more than that of the Tigris River in Mosul and much higher than that in Baghdad. Also, on a global scale, these values of STP are considered high, especially during high flow. On the other hand, the larger grain gradation class that can be transported in the medium gravel constitutes less than 0.00005% of the STP. Furthermore, the results of STC computations clearly show that the suspended sediment is the dominant part of the STC and the bed material constitutes less than 0.002% of the STC of the total load. However, approximately 90% of a large percentage of the STC concerns the clay and very fine silt. In this paper, findings of the hydrodynamic model-based evaluation of the hydraulic characteristics and STC, as well as the conducted field and laboratory investigations, can sufficiently support the understanding and add to the knowledge of the aspects of flow and STC of already uninvestigated natural rivers.

Acknowledgment

The authors would like to thank the State Commission of Dams and Reservoirs (SCDR) of the Ministry of Water Resources (MoWR), Iraq, for their financial and material support. They also express deep gratitude to the head and staff of the Directorate of Water Resources in Salahaldin Province, Iraq, for their support in the field works. The authors are also grateful to the technical and faculty staff of the Civil Engineering Department at the University of Technology, Baghdad, Iraq, for their valuable support and scientific assistance.

Author contribution

Conceptualization, Ala H. N. and Ali S. A.; methodology, Ala H. N. and Jaafar S. M.; software, Ala H. N.; validation, Ala H. N., and Jaafar S. M.; formal analysis, Ala H. N.; investigation, Ala H. N. and Jaafar S. M.; resources, Ala H. N.; data curation, Ala H. N.; writing original draft preparation, Ala H. N.; writing review and editing, Ali S. A. and Jaafar S. M.; visualization, Ala H. N.; supervision, Ali S. A. and Jaafar S. M.; funding acquisition, Ala H. N. All authors have read and agreed to the published version of the manuscript.

Funding

This research was funded by the Ministry of Water Resources, Iraq, Contract No. 1/Study/Dams/2021.

Data availability statement

The data that support the findings of this study are available from the corresponding author upon reasonable request. However, IMoWR (2021) [Documented Data] is unpublished data available at the Salahaldin Directorate of Water Resources, MoWR, Iraq. It can be received upon an official request.

Conflicts of interest

The authors declare no conflict of interest.

References

- [1] G.H. Merten, M.A. Nearing, A.L. Borges, Effect of sediment load on soil detachment and deposition in rills, *Soil Sci. Soc. Am. J.*, 65 (2001) 861–868. <https://doi.org/10.2136/sssaj2001.653861x>
- [2] H. Chanson, *The hydraulics of open channel flow*, New York, New York: John Wiley and Sons, 1999.
- [3] S.C. Finkner, M.A. Nearing, G.R. Foster, J.E. Gilley, A Simplified Equation for Modeling Sediment Transport Capacity, *Biosyst. Eng.*, 120 (1989) . <https://doi.org/10.13031/2013.31187>

- [4] N. Aziz, S. Prasad, Sediment Transport in Shallow Flows, *J. Hydraul. Eng.*, 111 (1985).
- [5] I. Celik, W. Rodi, Suspended sediment-transport capacity for open channel flow, *J. Hydraul. Eng.*, 117 (1991).
- [6] C. Yang, S. Wan, Comparisons of selected bed material load formulas, *J. Hydraul. Eng.*, 117 (1991).
- [7] Y. Shu-Qing, Sediment transport capacity in rivers, *J. Hydraul. Res.*, 42 (2005) 131–138. <https://doi.org/10.1080/00221686.2005.9641229>
- [8] M. Ali, G. Sterk, M. Seeger, M. Boersema, P. Peters, Effect of hydraulic parameters on sediment transport capacity in overland flow over erodible beds, *Hydrol. Earth Syst. Sci.*, 16 (2012) 591–601. <https://doi.org/10.5194/hess-16-591-2012>
- [9] N.T. McPherson, Identifying sediment transport potential and velocity profiles in the Carmel River using an ADP. Ph.D. thesis, Naval Postgraduate School, Monterey, California, USA, 2020.
- [10] K. Zhang, W. Xuan, B. Yikui, X. Xiuquan, Prediction of sediment transport capacity based on slope gradients and flow discharge. *PLoS. ONE.*, 16 (2021). e0256827. <https://doi.org/10.1371/journal.pone.0256827>
- [11] M. S. Al-Khafaji, A. S. Abbas, R. I. Abdulridha, Effect of Floating Debris on Local Scour at Bridge Piers, *Eng. Technol. J.*, 34 (2016) 356-367.
- [12] J. S. Maatooq, G. A. Kadhim, Evaluation of the Hydraulic Performance Indicators for Al- Ibrahim Irrigation Canal in the South of Iraq, *Eng. Technol. J.*, 34 (2016) 623-635. <http://dx.doi.org/10.30684/etj.34.3A.16>
- [13] T. S. Kayyun, H. M. Hadi, Modeling of Micro Hydroelectric Power Plants Utilizing Artificial Falls (Weirs) on Reach of Tigris River-Iraq, *Eng. Technol. J.*, 34 (2016) 2106-2122. <http://dx.doi.org/10.30684/etj.34.11A.16>
- [14] A. Molinas, B. Wu, Transport of sediment in large sand-bed rivers, *J. Hydraul. Res.*, 39 (2001).
- [15] A. H. Nama, Estimating the sediment transport capacity of Tigris River within Al Mosul City, *J. Eng.*, 17 (2011) 473–485.
- [16] J. Kim, P.Y. Julien, U. Ji, J. Kang, Restoration modeling analysis for abandoned channels of the Mangyeong River, *J. Environ. Sci.*, 20 (2011) 555-564. <http://dx.doi.org/10.5322/JES.2011.20.5.555>
- [17] R. Hummel, J. Duan, S. Zhang, Comparison of unsteady and quasi-unsteady flow models in simulating sediment transport in an ephemeral Arizona stream, *J Am Water Resour Assoc*, 48 (2012) 987–998. <https://doi.org/10.1111/j.1752-1688.2012.00663.x>
- [18] Jayshree T., S.M. Yadav, S. Waikhom, Estimating the sediment transport capacity using HEC-RAS, *GJRA.*, 2 (2013) 94-99.
- [19] S. I. Khassaf, Mohammed j.A., Modeling of sediment transport upstream of Al-Shamia Barrage, *Int. j. sci. eng.*, 6 (2015) 1338-1344. <https://www.citefactor.org/journal/pdf/Modeling-of-Sediment-Transport-Upstream-of-Al-Shamia-Barrage.pdf>
- [20] H. Abduljaleel, M.S. Al-Khafaji, A.H Nama, Sediment transport capacity of Tigris River within Baghdad City, *Int. J. Environ. Sustain. Dev.*, 5 (2016) 97–107.
- [21] H.S. Mohammed, A.M.U Alturfı, M.A. Shlash, Sediment transport capacity in Euphrates River at Al-Abbasia Reach using HEC-RAS model. *Int. J. Civ. Eng.*, 9 (2018) 919-929.
- [22] T.S. Kayyun, D.H. Dagher, Potential sediment within a reach in Tigris River, *J. Hydraul. Eng.*, 7 (2018) 22-32. <https://doi.org/10.5923/j.ijhe.20180702.02>
- [23] M.H. Daham, B.S. Abed, Simulation of sediment transport in the Upper Reach of Al-Gharraf River. *International Conference on Geotechnical Engineering-Iraq*, OP Conf. Series: Mater. Sci. Eng., 901,2020,012012. <https://doi.org/10.1088/1757-899X/901/1/012012>
- [24] W.A. Jassam, B. S. Abed, Assessing of the morphology and sediment transport of Diyala River, *J. Engineering*, 27 (2021) 47-63. <https://doi.org/10.31026/j.eng.2021.11.04>
- [25] V.K. Sissakian, S.F.A. Fouad, H.A. Al-Musawi, The influence of unstable slopes on the Stability of makhool dam – central Iraq, *Iraqi Bulletin of Geology and Mining*, 2 (2006) 31 – 44.
- [26] M. Al-Murib, Application of CE-QUAL-W2 on Tigris River in Iraq. Master Of Science in Civil and Environmental Engineering, Portland State University, 2014.
- [27] SCCCES (Swiss Consultants Consortium for Consulting Engineering Services), Study of operation of fatha dam and lake Tharthar and Optimization of Dam Height, 1985.
- [28] USACE (U.S. Army Corps of Engineers), River Analysis System, Version 5.0.6, Hydrologic Engineering Center, Davis CA 95616, (2005).
- [29] J.B. Fripp, P. Diplas, Surface sampling in gravel streams. *J. Hydraul. Eng.* X1993.119:473-490, by, ASCE (1993).

- [30] J.B.Laronne, I. Reid, Y. Yitshak, L.E. Frostick, The non-layering of gravel streambeds under ephemeral flood regimes. *J. Hydrol.*, 159 (1994.) 353-363.
- [31] V.T. Chow, *Open-channel hydraulics*: New York, McGraw-Hill,1959.
- [32] C. Santhi, J.G. Arnold, J.R. Williams, W.A. Dugas, R. Srinivasan, L.M. Hauck, Validation of the SWAT model on a large river basin with point and nonpoint sources. *JAWRA.*, 37(2001) 1169-1188.
- [33] D. N. Moriasi, J.G. Arnold, M.W. Van Liew, R.L. Bingner, R.D. Harmel, T.L. Veith, Model evaluation guidelines for systematic quantification of accuracy in watershed simulations. *Transactions of the American Society of Agricultural and Biological Engineers (ASABE)*, 50 (2007) 885–900.
- [34] K. Kuntiyawichai, W. Sri-Amporn, C. Pruthong C. Quantifying consequences of land use and rainfall changes on maximum flood peak in the lower Nam Pong River basin, *Adv. Mat. Res.*, 931-932 (2014)791-796. <https://doi.org/10.4028/www.scientific.net/AMR.931-932.791>
- [35] P. Jiao, D. Xu, S. Wang, Y. Yu, S. Han, Improved SCS-CN method based on storage and depletion of antecedent daily precipitation, *Water. Resour. Manage.*, 29 (2015) 4753-4765. <https://doi.org/10.1007/s11269-015-1088-6>
- [36] H. Akay, B. Koçyiğit, A.M. Yanmaz, a case study for determination of hydrological parameters in HEC-HMS in computing direct runoff. 12th International Congress on Advances in Civil Engineering (ACE) at Istanbul,2016.
- [37] Nearing, M. A., Foster, G. R. & Lane, L. J. A process-based soil erosion model for USDA-water erosion prediction project technology, *Trans ASAE*. 32, 1587–1593 (1989).
- [38] T.W. Lei, M.A. Nearing, K. Haghghi, V.F. Bralts, Rill erosion and morphological evolution: A simulation model. *Water Resour Res.*, 34 (1998), 3157–3168.
- [39] Z. Majeed , A.S. Abbas, I.A. Alwan, water flow simulation of Tigris River between Samara and Baghdad based on HEC-RAS model. *Eng. Technol. J.*, 39 (2021) 1882-1893. <http://doi.org/10.30684/etj.v39i12.1804>
- [40] R. J. Zhang, J. H. Xie, W.B. Chen, *River Mechanics*. China: Wuhan University Press in Chinese, 2007.
- [41] Y.H. Jia, Z.Y. Wang, X.M. Zheng, Y.F. Li, A study on limit velocity and its mechanism and implications for natural rivers. *Int. J. Sediment Res.*, 31(2016) 205-211. <https://doi.org/10.1016/j.ijsrc.2015.01.002>
- [42] C.T Yang, *Sediment Transport: Theory and Practice*. McGraw-Hill, New York,1996.
- [43] L.C. Rijn, *Principles of Sediment Transport in Rivers, Estuaries, Coastal Seas and Oceans*. International Institution for Infrastructural, Hydraulic, and Environmental Engineering. Delft, Netherlands ,1993.